Available online at www.sciencedirect.com
SCIENCE DIRECT®
Acta Materialia 52 (2004) 833–840
Acta MATERIALIA
www.actamat-journals.com

Quantitative interface models for simulating microstructure evolution

J.Z. Zhu *, T. Wang, S.H. Zhou, Z.K. Liu, L.Q. Chen

Department of Materials Science and Engineering, Penn State University, 106 Steidle Building, University Park, PA 16802, USA

Received 27 May 2003; received in revised form 22 September 2003; accepted 13 October 2003

Abstract

To quantitatively simulate microstructural evolution in real systems, we investigated three different interface models: a sharp-interface model implemented by the software DICTRA and two diffuse-interface models which use either physical order parameters or artificial order parameters. A particular example is considered, the diffusion-controlled growth of a γ' precipitate in a supersaturated γ matrix in Ni–Al binary alloys. All three models use the thermodynamic and kinetic parameters from the same databases. The temporal evolution profiles of composition from different models are shown to agree with each other. The focus is on examining the advantages and disadvantages of each model as applied to microstructure evolution in alloys.

Keywords: Phase-field models; Ni-base alloys; CALPHAD; Thermodynamics; Kinetics

1. Introduction

There have been significant advances in recent years in modelling the interface formation and motion during solid-state phase transformations and the subsequent microstructure coarsening processes employing various computation models. There are generally two types of approaches for treating the interfaces: the sharp-interface description [1–4] and the diffuse-interface description [5–7].

In a sharp-interface description, different phases are modelled as distinct regions in space separated by interfaces with zero thickness. For a diffusion-controlled process, microstructure evolution is modelled by solving the non-steady state diffusion equation with appropriate boundary conditions specified at the interfaces. Typical boundary conditions assume a local equilibrium coupled with mass conservation conditions.

An alternative to the sharp-interface modelling is the phase-field method which describes a microstructure using a set of physical and/or phase-field variables. The interfaces are represented by diffuse regions with a certain thickness where the phase-field variables change continuously. Complex two- (2D) and three-dimensional (3D) microstructures can be easily modelled since there is no need to explicitly track the interfaces. There are basically two types of phase-field models. In the first type, the field variables, also known as the phase-fields, are introduced for the sole purpose of avoiding tracking the interfaces. The thermodynamic and kinetic coefficients in a phase-field model are then chosen to fit the corresponding parameters in the conventional sharp- or thin-interface equations through asymptotic analysis. In the second type, the field variables correspond to well-defined physical order parameters such as long-range order parameters for order–disorder transformations and the composition fields for phase separation. Both these two types of models assume that the microstructure evolution during a given process is governed by the phase-field equations, and in principle, all the thermodynamic and kinetic coefficients can be related to microscopic parameters.

Phase-field methods have been applied to a wide range of microstructural evolution problems including grain growth, spinodal decomposition, ordering and antiphase domain coarsening, solidification, ferroelectric domain formation, martensitic transformation and precipitation under applied stress [6,7]. It has been

* Corresponding author. Tel.: +1-814-865-0389; fax: +1-814-865-2917.
E-mail address: zhu@ems.psu.edu (J.Z. Zhu).

1359-6454/$30.00 © 2003 Acta Materialia Inc. Published by Elsevier Ltd. All rights reserved.
doi:10.1016/j.actamat.2003.10.017

demonstrated that the microstructures predicted from phase-field simulations show remarkable agreement with experimental observations, at least qualitatively as long as the model incorporates the essential thermodynamic and kinetic features for a given process. However, despite its great progress, the phase-field model has not been established as a computational tool which can routinely take the real thermodynamic and kinetic parameters as input and predict the quantitative microstructure evolution although a number of attempts have been made in this direction [8–10].

The main purpose of this paper is to examine two different types of phase-field models: a model based on the physical order parameters which we call the physical model and that based on artificial order parameters which is similar to the KKS model [11,12] by quantitatively studying the microstructural evolution using thermodynamic and kinetic parameters directly from existing databases and by comparing the kinetics of microstructure evolution obtained from the DICTRA code based on a sharp-interface description. Specifically we investigated the one-dimensional (1D) diffusion-controlled growth of a γ' precipitate from the supersaturated γ matrix in a Ni–Al binary system. The focus of the discussion is on the advantages and disadvantages of each model as applied to microstructure evolution in alloys.

2. Models

2.1. Thermodynamic and atomic mobility descriptions

A typical microstructure of Ni-base alloys consists of a dispersion of ordered intermetallic precipitate particles of the type $L1_2$ (γ') embedded in a fcc matrix (γ). According to Ansara et al. [13], the molar Gibbs free energy G_m is modelled by a two sub-lattice model as follows:

$$G_m = G_m^{dis}(x_i) + G_m^{ord}(y_i', y_i'') - G_m^{ord}(x_i), \tag{1}$$

where x_i is the composition of component i, and y_i', y_i'' are the two site fractions of component i in the different sub-lattices. $G_m^{dis}(x_i)$ is the Gibbs free energy of the disordered state, $G_m^{ord}(y_i', y_i'')$ is the Gibbs energy described by the sub-lattice model and $G_m^{ord}(x_i)$ is the energy contribution of the disordered state to the ordered state. The free energy describing both ordered phase and disordered phases are evaluated independently and compiled into thermodynamic Thermo-Calc databases which include phase constituents, reference states of elements and interaction parameters.

The database for the atomic mobility of species in individual phases is constructed to obtain the kinetic information of a microstructural evolution. In particular for the diffusion-controlled process in our study, the diffusion in the ordered $L1_2$ phase is ignored and the diffusional mobility in the fcc phase is considered as the main factor determining the kinetics. Assuming diffusion occurs through the vacancy exchange mechanism and all elements are substitutional, the intrinsic diffusion coefficient, D_{kj} (the diffusivity of component k with respect to the gradient of component j), is related to the atomic mobility M_i (i for all the elements in a phase) as [14,15],

$$D_{kj} = \sum_{i=1}^{n} (\delta_{ik} - x_k) x_i M_i \frac{\partial \mu_i}{\partial x_j}, \tag{2}$$

where δ_{ik} is the Kronecker-delta function and μ_i is the chemical potential of component i derived from the Gibbs energy of the phase. The quantity $\partial\mu_i/\partial x_j$ defined the thermodynamic factor which can be evaluated from the thermodynamic database. M_i in the database is assessed from the tracer or self-diffusion coefficient D_i^* by $M_i = D_i^*/(RT)$ which is determined from experimental diffusion studies using isotopes.

2.2. DICTRA simulations based on the sharp-interface description

In the sharp-interface model, a local equilibrium at the moving interface between γ and γ' phases is assumed. The multicomponent diffusion equation in each phase needs to be solved

$$\begin{aligned} J_k &= -\sum_{j=1}^{n-1} \tilde{D}_{kj}^n \nabla c_j, \\ \frac{\partial c_k}{\partial t} &= -\mathrm{div}(J_k), \end{aligned} \tag{3}$$

where J_k is the diffusional flux of element k, $\tilde{D}_{kj}^n$ represents the interdiffusion coefficient matrix calculated from atomic mobilities [15], and ∇c_j is the concentration gradient. The phase interface migration is determined by the flux-balance equation for conserving the number of moles of a component k as [4]

$$v^{\gamma}(c_k^{\gamma} - c_k^{\gamma'}) = J_k^{\gamma} - J_k^{\gamma'}, \quad k = 1, 2, \ldots, n, \tag{4}$$

where v^{γ} is the interface migration rate, c_k^{γ} and $c_k^{\gamma'}$ are the concentrations of component k in γ and γ' close to the phase interface, and J_k^{γ} and $J_k^{\gamma'}$ are the corresponding diffusional fluxes.

The simulation of 1D diffusion-controlled growth is carried out by using the software DICTRA (DIffusion Controlled TRAnsformations in multicomponent alloys). DICTRA is linked with Thermo-Calc software, which provides all necessary thermodynamic calculations [3,4].

2.3. Phase-field model with physical order parameters

In this model, two sets of field variables, i.e., the local composition c of alloy species and a three-component

physical long-range order parameter field (η_1, η_2, η_3) were used to describe $\gamma + \gamma'$ two-phase microstructures. The composition field specifies the local compositional distributions of all the species and the long-range order parameter field describes the four types of possible $L1_2$ ordered domains related by a lattice translation and distinguishes the structural difference between ordered precipitates and the disordered matrix related by the $L1_2$ ordering. The three-component order parameter is selected to represent fcc $\rightarrow L1_2$ ordering based on atomic site locations [16–18]. Thus the order parameters η_i ($i = 1, 2, 3$) are physical parameters which can be associated with the site fractions y_i' and y_i'' as introduced in the thermodynamic database. We refer this model as the physical model.

Considering Eq. (1) which describes the total Gibbs energy in terms of the composition and two site fractions by a two sub-lattice model in the thermodynamic database, we have employed a four sub-lattice model with Ni and Al soluble in each sub-lattice to model the total Gibbs free energy as

$$G_{\mathrm{m}} = G^{\mathrm{dis}}(c) + G^{\mathrm{ord}}(c, \eta_1, \eta_2, \eta_3) - G^{\mathrm{ord}}(c, \eta_i = 0), \qquad (5)$$

where each term has essentially the same meaning as in Eq. (1). Details of formulating Eq. (5) in terms of composition and order parameters can be found in [19] where we have obtained a complete Gibbs free energy description of both phases in Ni-base alloys by linking to the thermodynamic database. The Gibbs free energy G_{m} in the unit of J/mol obtained from the thermodynamic database is then converted to the free energy density $f(c, \eta_i)$ in the unit of J/m^3 by the molar volume V_{m} as $f(c, \eta_i) = G_{\mathrm{m}}/V_{\mathrm{m}}$.

In order to compare with the results by DICTRA simulations which do not include the elastic energy calculation, we consider a Ni–Al system at a high temperature when the lattice mismatch between precipitate and matrix is so small that the elastic energy contribution can be ignored. The general form for the total stress-free chemical free energy in the phase-field model is [20]

$$F = \int_V \left[f(c, \eta_i) + \frac{\alpha}{2}(\nabla c)^2 + \sum_{p=1}^{3} \frac{\beta_{ij}(p)}{2} \nabla_i \eta_p \nabla_j \eta_p \right] \mathrm{d}V, \qquad (6)$$

where $\nabla_i = \partial/\partial x_i$ is the ith component of the vector operator ∇ and x_i is the ith component of the spatial coordinate vector. In Eq. (6), α and $\beta_{ij}(p)$ are gradient energy coefficients that control the diffuse-interface thickness and interfacial energies. The gradient energy coefficient for the orientation field variables $\beta_{ij}(p)$ is written in a tensor form so as to incorporate the interfacial energy anisotropy. An isotropic interfacial energy is assumed in the present work for simplicity.

Microstructural evolution is assumed to be governed by two sets of non-linear time-dependent field equations: the Cahn–Hilliard equation for the composition field and the Ginzburg–Laudau equation for the long-range order parameters [20,21]:

$$\frac{\partial c(\mathbf{r}, t)}{\partial t} = \nabla \cdot \left[M \nabla \frac{\delta F}{\delta c(\mathbf{r}, t)} \right], \qquad (7)$$

$$\frac{\partial \eta_i(\mathbf{r}, t)}{\partial t} = -L_i \frac{\delta F}{\delta \eta_i(\mathbf{r}, t)}, \quad i = 1, 2, 3, \qquad (8)$$

where c is the mole fraction of Al. L_i and M are the structural relaxation kinetic coefficient and the diffusion mobility, respectively. The diffusion mobility term M is related to the atomic mobilities of Ni and Al through $M = c_{\mathrm{Al}} c_{\mathrm{Ni}} [c_{\mathrm{Al}} M_{\mathrm{Ni}} + c_{\mathrm{Ni}} M_{\mathrm{Al}}]$, where M_{Ni} and M_{Al} are obtained from the atomic mobility database of fcc phase [15]. There is no direct experimental data available to determine the kinetic coefficient L_i for the structural order parameters. However, it can be approximated as a measure of the inverse of time it takes for the diffusing species to make a unit jump to its nearest neighbor sites in a fcc lattice. Following [22], the quantity of L_i is estimated using $M = L_i a_0^2/16$, where a_0 is the lattice parameter. It should be noted that an accurate quantity of L_i is not necessary in our particular study since the structural relaxation is much faster than diffusion and the interface migration velocity is mainly controlled by the diffusion mobility. We have developed an accurate and efficient semi-implicit Fourier spectral method for solving the two sets of kinetic equations [23].

Assuming the three-order parameter gradient coefficients are equal and isotropic, denoted as β, we can write the interfacial energy in one-dimension with the composition and order parameter inhomogeneity as [20]

$$\sigma = \int_{-\infty}^{\infty} \left[\Delta f(c, \eta_i) + \frac{\alpha}{2} \left(\frac{\mathrm{d}c}{\mathrm{d}x} \right)^2 + \frac{\beta}{2} \sum_i \left(\frac{\mathrm{d}\eta_i}{\mathrm{d}x} \right)^2 \right] \mathrm{d}x, \qquad (9)$$

where $\Delta f(c, \eta_i)$ is the free energy of the homogeneous alloy with respect to the free energy of the equilibrium two-phase mixture. The above equation means there are two contributions to the interfacial energy of a diffuse interface: the excess free energy term and the gradient terms. At equilibrium, the field variables, composition and/or order parameter, will vary in a way that the integral in Eq. (9) is minimized. A further analysis shows that the contribution of excess free energy term and the gradient terms to the total interfacial energy is equal at equilibrium [20]. Therefore, Eq. (9) can be simplified as $\sigma = 2 \int_{-\infty}^{\infty} \Delta f(c, \eta_i)\, \mathrm{d}x$. The gradient energy coefficients need to be determined to match the experimentally determined interfacial energy and anti-phase boundary energy.

2.4. Phase-field model with artificial order parameters

In this model, we adopted the phase-field formulation originally developed for studying the solidification of alloys [11,24,25]. A composition c and four artificial order parameter fields $(\phi_1, \phi_2, \phi_3, \phi_4)$ are used to distinguish the four types of ordered domains of the γ' phase and the disordered γ phase. These order parameters are artificial in a sense that they do not have direct physical meaning other than representing the ordered regions.

Since in this paper we only consider the growth of a single ordered precipitate in a disordered matrix in one dimension, one artificial order parameter is sufficient. The total free energy is written as

$$F = \int_V \left[f(c,\phi) + \frac{\varepsilon^2}{2}(\nabla\phi)^2 \right] \mathrm{d}V, \tag{10}$$

where ε^2 is the gradient energy coefficient of order parameter. The diffuse-interface region is regarded as a mixture of disordered phase and ordered phase with different compositions as in the KKS model [11,12],

$$c = h(\phi)c^p + (1-h(\phi))c^m, \quad f^p_{c^p}(c^p) = f^m_{c^m}(c^m), \tag{11}$$

where $h(\phi)$ is a monotonously changing function from $h(0) = 0$ and $h(1) = 1$. f^p is the chemical free energy of the precipitate phase and $f^p_{c^p}$ is the derivative of f^p with respect to c^p. f^m and $f^m_{c^m}$ follow similar meanings for the matrix phase. Therefore, the interface region is defined as a mixture of precipitate phase and matrix phase with the same chemical potential. In the KKS model, c^p and c^m are not the compositions of precipitate and matrix sides across the interface, but the compositions of the precipitate and matrix phases that make up the interface. Each point in the interface is considered as a mixture of c^p and c^m where Eq. (11) is satisfied.

The free energy density of the system $f(c,\phi)$ is defined as [11]

$$f(c,\phi) = h(\phi)f^p(c^p) + (1-h(\phi))f^m(c^m) + wg(\phi), \tag{12}$$

where $g(\phi)$ is the double-well potential associated with phase change and w is the double-well potential height. Following [26], we choose the functions $g(\phi) = \phi^2(1-\phi)^2$ and $h(\phi) = \phi^3(6\phi^2 - 15\phi + 10)$. Thermodynamic databases can provide us with the full description of the Gibbs free energies of both phases, f^p and f^m, as a function of composition at a given temperature. For given c and ϕ, theoretically c^p and c^m can be obtained by numerically solving Eq. (11). However, since the databases use non-linear description of the Gibbs free energy, numerical approximation has to be employed and it would be computationally intensive to find the numerical solutions of c^p and c^m. For simplicity, the free energy of both phases can be approximated as parabola functions whose first and second derivatives are imported from the thermodynamic databases. With a parabola approximation of the free energy density, c^p and c^m can be easily solved. Another solution is to tabulate the introduced variables c^p and c^m in terms of composition and order parameter by using the Gibbs free energy in the thermodynamic database. From our tests, no significant difference has been found for the solution of c^p and c^m between the parabola approximation and tabulation approach.

The evolution equations are written in a form similar to that used in [11]

$$\frac{\partial\phi}{\partial t} = -L\frac{\delta F}{\delta\phi} = L(\varepsilon^2\nabla^2\phi - f_\phi), \tag{13}$$

$$\frac{\partial c}{\partial t} = \nabla\cdot\left[\frac{\tilde{D}(c)}{f_{cc}}\nabla f_c\right], \tag{14}$$

where $\tilde{D}$ is the interdiffusion coefficient (or called chemical diffusion coefficient) obtained from the diffusion mobility of fcc phase by $\tilde{D} = M\frac{\mathrm{d}^2 f^m}{\mathrm{d}c^2}$ and $\frac{\mathrm{d}^2 f^m}{\mathrm{d}c^2}$ as well as f_{cc} are obtained from the thermodynamic database. The phase field mobility L can be estimated in a similar way as discussed in the physical model. Parameters ε^2 and w, which determine the interfacial width 2λ, need to be evaluated by the interfacial energy value σ. From the 1D equilibrium analysis, the interfacial energy σ can be calculated by $\sigma = \varepsilon^2\int_{-\infty}^{\infty}\left(\frac{\mathrm{d}\phi_0}{\mathrm{d}x}\right)^2\mathrm{d}x$, where ϕ_0 is the order parameter profile at the equilibrium state [27]. From the definition of interface energy and interface thickness, w and ε can be determined by $\sigma = \frac{\varepsilon\sqrt{w}}{3\sqrt{2}}$ and $2\lambda = \alpha\sqrt{2}\frac{\varepsilon}{\sqrt{w}}$, where α is a constant dependent on the definition of interface thickness 2λ [11].

3. Results

3.1. Equilibrium properties of interface

The equilibrium properties of the γ/γ' interface in the diffuse-interface models can be obtained by the evolution of an initial system with one interface separating two phases which have reached their equilibrium state. Fig. 1 shows the composition profile, order parameter profile and Gibbs free energy across an equilibrium γ/γ' interface obtained using the physical and the KKS models at 1300 K. Each symbol represents the corresponding values at the grid points. For the physical model, the gradient energy coefficients α and β are chosen as 3.6×10^{-9} J/m and 3.6×10^{-12} J/m, respectively. For the KKS model, $\varepsilon^2 = 5.6\times10^{-11}$ J/m and $w = 1.3\times10^8$ J/m^3. In both cases, the unit grid size $\mathrm{d}x = 0.1$ nm and the interfacial energy $\sigma = 0.02$ J/m^2 were used.

In Fig. 1(a) we observe a smooth change of the equilibrium composition value from $c_{\gamma'} = 0.2287$ in the γ' phase to $c_\gamma = 0.1595$ in the γ phase. The equilibrium

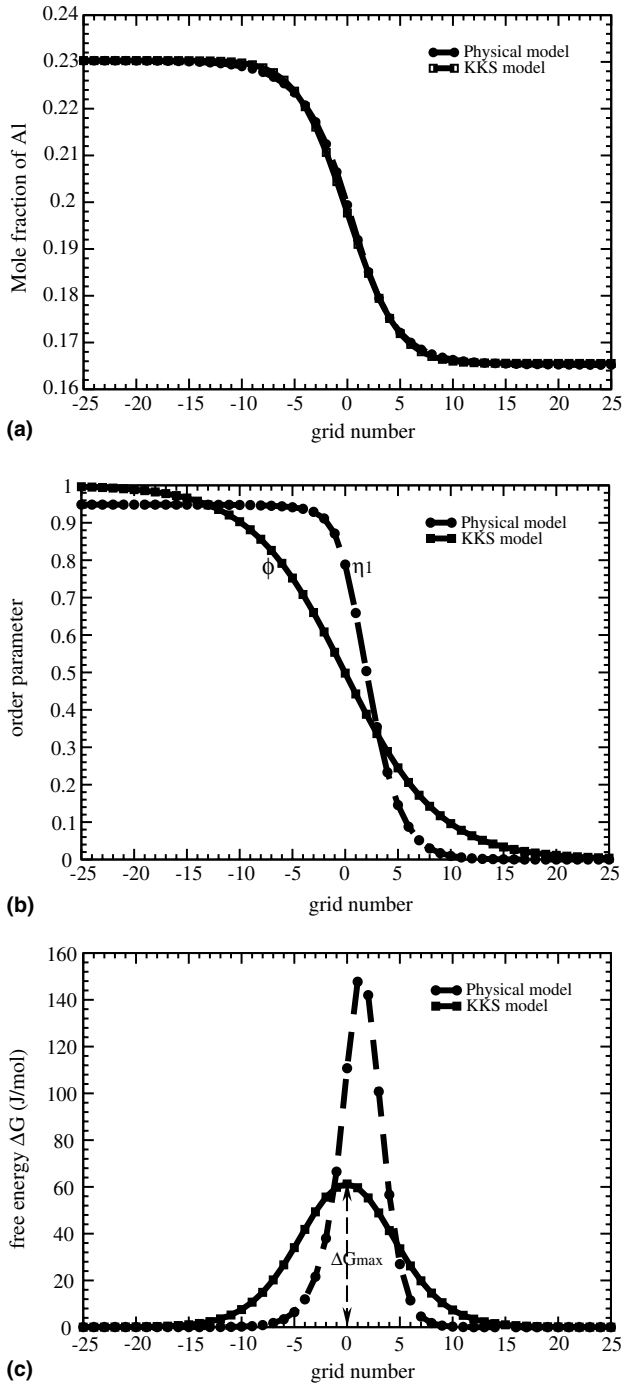

Fig. 1. The obtained composition, order parameter and free energy across the interface in the diffuse-interface models: (a) composition; (b) order parameter; (c) free energy ΔG_m.

composition profiles obtained by both models match each other very well. However, there is a significant difference of the order parameter profile between the results obtained by two models as shown in Fig. 1(b). In the physical model, the equilibrium values of the composition and order parameters, predetermined by the minimization of the free energy with respect to the composition and order parameters, are automatically obtained through the solution of phase-field equations. In the KKS model, the order parameter equilibrium value is 0 for disordered phase and 1 for ordered phase determined by the double well function $g(\phi)$. An analytical solution exists for the equilibrium order parameter profile which is given by [28] as $\phi_0(x) = \frac{1}{2}[1 - \tanh(\frac{\sqrt{w}}{\sqrt{2}\varepsilon}x)]$. The solid line obtained by the KKS model simulation in Fig. 1(b) agrees exactly with this analytical solution. Fig. 1(c) shows the free energy densities ΔG_m obtained by Eqs. (5) and (12) where the common tangent line is subtracted, i.e., with the equilibrium mixture of γ and γ' as the reference state. It can be seen that the KKS model has a wider interface and lower maximum ΔG_{max} for the same fixed interfacial energy.

The integral of the free energy ΔG_m with respect to the position along the interface, i.e., the area under the curve in Fig. 2(c), is equal to half of the interface energy σ. The interfacial width 2λ can thus be roughly estimated from the interfacial energy σ and the free energy maximum ΔG_{max} by $2\lambda \approx \sigma V_m/\Delta G_{max}$. In the physical model, the interfacial width is a physical property describing the thickness of the region separating the two phases. With σ obtained from experimental results and ΔG_{max} estimated from the free energy description in the thermodynamic database, the interfacial width 2λ is thus determined. Therefore, the interfacial width in the physical model is independent of the unit grid size dx. In the numerical grids, the number of points N representing the diffuse-interface is roughly proportional to $2\lambda/\mathrm{d}x$. Thus, the larger dx, the less N in the interface. However, since there must be a minimum N (usually 4–5 points) in the interface to maintain numerical accuracy and stability, the maximum unit grid size, and consequently the maximum system size the physical model can handle, are therefore limited by the physical interfacial width. For example, taking the γ/γ' interfacial energy value $\sigma = 0.02$ J/m^2, $\Delta G_{max} = 160$ J/mol at 1300 K and the molar volume $V_m = 7 \times 10^{-6}$ m^3/mol, we estimate the interfacial

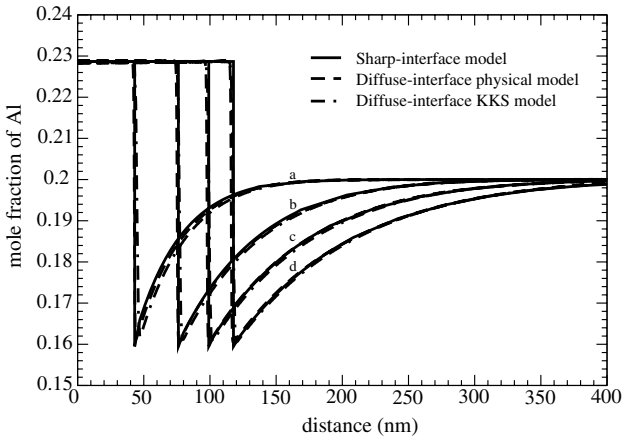

Fig. 2. Temporal evolution of composition profiles obtained by different models: (a) $t = 0.1$ s; (b) $t = 0.3$ s; (c) $t = 0.5$ s; (d) $t = 0.7$ s.

width $2\lambda \approx 1$ nm. Assuming there are 5 points to resolve the interface, dx is thus 0.2 nm.

In the KKS model, the interface is no longer a physical entity, but an artificially introduced region for technical convenience as mentioned earlier [11]. The double well potential function $g(\phi)$ is also artificially introduced to obtain the ordered and disordered equilibrium phases. The double well potential height w in Eq. (12), representing the maximum free energy $\Delta G_{\max}$ in Fig. 1(c), determines the interfacial width 2λ for a given interfacial energy. The parameter w is selected dependent on the interfacial width. Therefore there is one degree of freedom in either w or 2λ to match a fixed interfacial energy. Much thicker interface can be chosen with a smaller w without fundamentally altering the physical properties under consideration. As a result, larger unit grid size dx can be used than that in the physical model.

3.2. Kinetics of interface motion

The interface models were used to simulate the diffusion-controlled growth of a γ' precipitate in a disordered γ matrix in the Ni–Al binary system at 1300 K and the average mole fraction of Al $c_0 = 0.2$. The system size is 2 μm. For the sharp-interface model implemented by DICTRA, the initial composition is a constant everywhere throughout the system. A nucleus with size 0.1 nm is introduced at time $t > 0$. It is noted that since the interfacial energy contribution to the total free energy is not included in the DICTRA simulation, any size of new phase particle will grow, i.e. the critical size is zero. For the initial configuration in the diffusion-interface models, a precipitate with equilibrium composition and/or order parameter values is placed in the middle of the disordered matrix with a periodic boundary condition.

Fig. 2 shows the simulated growth of a γ' precipitate by plotting the composition profiles as a function of time obtained by different models. For the DICTRA simulation, an initial time step dt of 10^{-7} s is used and adaptive time step followed by adaptive time steps. Based on the local equilibrium hypothesis, the compositions at the sharp-interface always assume the equilibrium values $c_{\gamma'} = 0.2287$ and $c_{\gamma} = 0.1595$ at 1300 K. As seen in the solid lines in Fig. 2, the composition everywhere in the precipitate is constant $c_{\gamma'}$ and has a sharp change c_{γ} at another side of the interface.

The diffuse-interface model simulations agree well with the results from DICTRA as seen by the dashed line (the physical model) and dot-dashed line (the KKS model) in Fig. 2 except that the compositions change continuously with values close to the equilibrium compositions across the interface. An interfacial energy value $\sigma = 0.02$ J/m^2 was used. Since the precipitation process is driven by the bulk free energy reduction, the magnitude of the interfacial energy has no effect on the kinetics but determines how many points existing across the interface. In the physical model simulation, the unit grid size dx is 0.325 nm and the time step is 10^{-7} s. The gradient energy coefficients α and β are determined to be 3.8×10^{-9} J/m and 5.6×10^{-12} J/m, respectively. The following parameters are selected for the KKS model simulation: d$x = 1$ nm, d$t = 5 \times 10^{-6}$ s, $w = 6.6 \times 10^{7}$J/m^3 and $\varepsilon^2 = 1.1 \times 10^{-10}$ J/m.

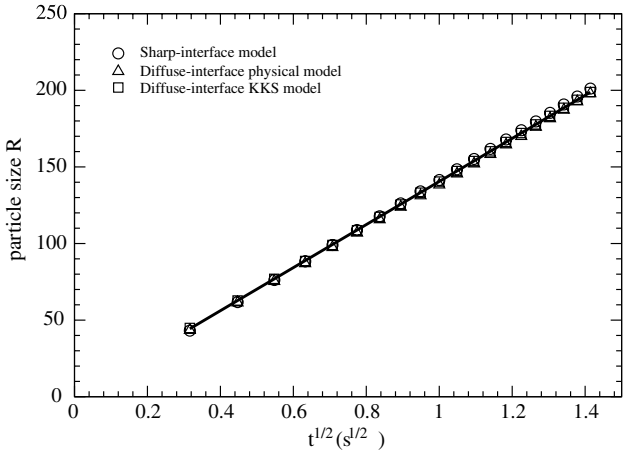

Fig. 3. A parabolic growth of the precipitate size R as a function of square root of time $t^{1/2}$ in the diffusion-controlled growth.

For a diffusion-controlled growth, it is well known that the precipitate grows with time according to a parabolic growth law as

$$R = K(Dt)^{1/2}, \tag{15}$$

where R is the precipitate size and K is the rate constant. The parabolic growth behavior is validated by the plot in Fig. 3 where the interface position as a function of the square root of time is shown. The data agree with each other and can be fit into a straight line in all three different models.

4. Discussions

In the sharp-interface model, a phase transformation is governed by diffusion and curvature (Gibbs–Thomson effect). The interface motion velocity is determined from a local mass balance and a calculation of the curvature. For 1D simulation, the curvature effect is zero and microstructural evolution is modelled by tracking the interface. In this paper, the software package DICTRA was used for the sharp-interface simulation. Compared with the other two diffuse-interface models, DICTRA simulation is much simpler and at least one order of magnitude faster but is only limited to simple 1D (planar, cylindrical and spherical) geometries.

The diffuse-interface phase-field models overcome the difficulties of tracking phase boundaries of the sharp-interface model and can be easily extended to 2D and 3D systems. Elastic effects can also be incorporated to

the phase-field physical model [29]. The interfacial energy anisotropy can be incorporated in a natural and physical way [30]. Therefore, most of the morphological transformations in coherent solids can be satisfactorily explained.

However, the physical system size and evolution time are rather limited due to the nature of the physical model. As mentioned earlier, since all the order parameters are physical, the interfacial width is also a physical width determined by the chemical free energy and the interfacial energy. In order to describe the microstructure evolution kinetics accurately, a certain number of grid points are required to resolve an interface. With a uniform grid, the total system size is limited by the total number of grid points. For example, the interfacial width of Ni–Al binary system in this model is approximately 1 nm at 1300 K as estimated in the previous section. With at least 5 points to resolve the interface, the unit grid size is 0.2 nm and the corresponding time step is only about 10^{-7} s to maintain the numerical stability. Considering a real microstructure evolution in a scale of 1 μm and a coarsening time of 1 second, 5000^3 grid points in 3D and total time steps in the order of 10^7 are required. A simulation with such a large system size and computation time is still impossible to be practically carried out even with the most powerful parallel supercomputer currently available. Therefore, the simulations are often limited to small systems with length scale usually hundreds of nanometers 2D or tens of nanometers in 3D. Although such small system sizes might be sufficient during precipitate nucleation and growth, they are too small to obtain good statistics for coarsening kinetics.

Most thermodynamic and kinetic properties under consideration are treated in a similar way in the KKS model and the physical model. The main advantage of the KKS model is that the interface thickness can be adjusted by changing the double-well potential height to fit the actual interface energy. Thus, in principle, much wider interface thickness can be chosen, allowing us to increase the simulation system size significantly. Indeed, we found that the unit grid size in the KKS model could be at least one order of magnitude larger than that in the physical model.

However, there are also a number of disadvantages of the KKS model as compared to the physical model. First of all, the order parameters are not physical, so interfacial energy anisotropy, if required, has also to be introduced artificially through the orientation dependence of the gradient energy coefficient. Secondly, Eq. (11) has to be solved at each time step to obtain the two compositions that make up the interface. In general, numerical solutions could be computationally very expensive except for cases that a dilute solution model can be employed or the second derivatives of the free energy with respect to composition can be assumed to be constant. Finally, it is tricky to introduce the coherency elastic energy because of the assumption of a mixture of precipitate and matrix phases in the interfacial region and the additional difficulty in solving the coupled evolution equations when introducing coherency strain energy. In addition, due to the wider interface, the elastic field calculated around a precipitate with different interface widths will also be different.

5. Summary

Three different quantitative computational tools for modelling microstructure evolution have been investigated including a sharp-interface model using DICTRA and two diffuse-interface models which use either physical order parameters or artificial order parameters to describe the microstructure. By establishing links with existing thermodynamic and kinetic databases, we have compared each model by studying the diffusion-controlled growth of an ordered precipitate from a disordered matrix in a Ni–Al binary alloy. The interface property in the two diffuse-interface models has been compared by examining the composition, order parameter and free energy distribution across the interface. Quantitative comparisons about composition evolution profile and the growth kinetics show the feasibility of these quantitative models in predicting microstructural evolution. Each of the three models has its own advantages and disadvantages. The sharp-interface modelling implemented by DICTRA software is the most simple approach in obtaining quantitative kinetic information about a diffusion controlled transformation in many cases of interest. However, it is only limited to 1D. The diffuse-interface physical model offers us with a few advantages in that it uses the long-range order parameters as physical parameters to describe the microstructure and the free energy of different phases are constructed directly from the thermodynamic databases. It can be applied to phase transformations in 1D and has been applied successfully for quantitative simulations on relative small systems in 2D and 3D for relatively short times. Larger system and longer time simulation of complicated microstructures are possible to be carried out by the diffuse-interface KKS model which introduces artificial interface width for increasing the length scale of the system although a few difficulties exist including numerically solving a set of non-linear equations at each time step.

Acknowledgements

The authors are grateful for the financial support from NASA under Grant No. NCC3-920 and the computational resource award from NCSA under grant

no. DMR030004N and DMR020002P. Simulations were performed in NCSA Linux cluster and Pittsburgh Supercomputing Center T3E.

References

[1] Fratzl P, Penrose O, Lebowitz JL. J Stat Phys 1999;95:1429.
[2] Jou HJ, Leo PH, Lowengrub JS. J Comput Phys 1997;131:109.
[3] Andersson JO, Helander T, Hoglund L, Shi PF, Sundman B. CALPHAD 2002;26:273.
[4] Borgenstam A, Engstrom A, Hoglund L, Agren J. J Phase Equilib 2000;21:269.
[5] Cahn JW. Acta Metall 1961;9:795.
[6] Chen LQ, Wang YZ. Jom 1996;48:13.
[7] Chen LQ. Annu Rev Mater Res 2002;32:113.
[8] Loginova I, Odqvist J, Amberg G, Agren J. Acta Mater 2003;51:1327.
[9] Karma A. Phys Rev Lett 2001;87:115701.
[10] Cha PR, Yeon DH, Yoon JK. Acta Mater 2001;49:3295.
[11] Kim SG, Kim WT, Suzuki T. Phys Rev E 1999;60:7186.
[12] Cha PR, Yeon H, Yoon K. unpublished paper.
[13] Ansara I, Dupin N, Lukas HL, Sundman B. J Alloy Compd 1997;247:20.
[14] Andersson JO, Agren J. J Appl Phys 1992;72:1350.
[15] Campbell CE, Boettinger WJ, Kattner UR. Acta Mater 2002;50:775.
[16] Lai ZW. Phys Rev E 1990;41:9239.
[17] Wang Y, Banerjee D, Su CC, Khachaturyan AG. Acta Mater 1998;46:2983.
[18] Vaithyanathan V, Chen LQ. Scr Mater 2000;42:967.
[19] Zhu JZ, Liu ZK, Vaithyanathan V, Chen LQ. Scr Mater 2002;46:401.
[20] Cahn JW, Hilliard JE. J Chem Phys 1958;28:258.
[21] Allen SM, Cahn JW. Acta Metall 1979;27:1085.
[22] Poduri R, Chen LQ. Acta Mater 1998;46:3915.
[23] Zhu JZ, Chen LQ, Shen J, Tikare V. Phys Rev E 1999; 60:3564.
[24] Wheeler AA, Boettinger WJ, McFadden GB. Phys Rev A 1993;45:7424.
[25] Tiaden J, Nestler B, Diepers HJ, Steinbach I. Physica D 1998;115:73.
[26] Warren JA, Boettinger WJ. Acta Metall 1995;43:689.
[27] Wheeler AA, Boettinger WJ, McFadden GB. Phys Rev E 1993;47:1893.
[28] Kim SG, Kim WT, Suzuki T. Phys Rev E 1998;58:3316.
[29] Chen LQ. In: Phase Transformations and Evolution in Materials. Warrendale, PA: TMS; 2000. p. 209.
[30] Taylor JE, Cahn JW. Physica D 1998;112:381.